

Electronic Supporting Information

Synthesis, Characterization and Photoinduced Charge

Separation of Carbon Nanohorn-Oligothiénylenevinylene

Hybrids

María Vizuete,^a María J. Gómez-Escalonilla,^a Myriam Barrejón,^a José Luis G. Fierro,^b
Minfang Zhang,^c Masako Yudasaka,^c Sumio Iijima,^{c,d} Pedro Atienzar,^e Hermenegildo
García^{e*} and Fernando Langa^{a*}

^a *Universidad de Castilla-La Mancha, Instituto de Nanociencia, Nanotecnología y Materiales
Moleculares (INAMOL), 45071, Toledo, Spain.*

E-mail: Fernando.langa@uclm.es

^b *Instituto de Catálisis y Petroleoquímica, CSIC, Cantoblanco, 28049, Madrid, Spain.*

E-mail: jlqfierro@icp.csic.es

^c *Nanotube Research Center, National Institute of Advanced Industrial and Technology, Higashi,
Tsukuba, Ibaraki 305-8565, Japan.*

E-mail: m-yudasaka@aist.go.jp

^d *Department of Physics, Meijo University, Shiogamaguchi, Tenpakuku,*

Nagoya 468-8502, Japan

^e *Instituto Universitario de Tecnología Química CSIC-UPV,*

Universidad Politécnica de Valencia, 46022, Valencia, Spain.

E-mail: hgarcia@qim.upv.es

<u>Table of Contents</u>	<u>Page</u>
Instrumentations	S3
TGA curves Figure S1	S6
Functionalization data Table S1	S7
XPS spectra Figures S2-S5	S8
XPS data Table S2	S10
Structures of 2TV(1) and 4TV (2) Scheme S1.	S11
Electrochemistry Figure S6 and Table S3	S12
Absorption spectrums of compounds 1 and 3 with MV and MeOH, irradiating with 355 nm laser excitation.	S13
Transients spectra of compounds 2 and 4 at 532 nm	S14

Instrumentation. Raman measurements were carried out at room temperature using a Renishaw in Via Raman microscope equipped with a CCD camera and a confocal Leica microscope. As an excitation source 532 laser was employed. The sample was measured on a glass substrate as powder. Measurements were taken with 10 seconds of exposure times at varying number of accumulations. The laser spot was focused on the sample surface using a long working distance 50x objective. All spectra were recorded over several regions and were referenced to the silicon line at 520 cm^{-1} . The intensity ratio I_D/I_G was obtained by taking the peak intensities after baseline correction. The data was collected and analysed with Renishaw Wire and origin software. XPS measurements were performed using a VG Escalab 200R electron spectrometer equipped with a Mg $K\alpha$ x-rays ($h\nu = 1254.6\text{ eV}$) source and a spherical section analyzer. The instrument has five element multichannel detectors. The X-ray beam used was a 120 W, 240 μm diameter beam. The X-ray beam was incident normal to the sample and the photoelectron detector was at 45° off-normal. Wide scan data was collected using pass energy of 100 eV. For the Ag3d5/2 line, these conditions produce FWHM of better than 1.8 eV. Narrow scan or high energy resolution spectra were collected using pass energy of 20 eV. The binding energy (BE) scale was calibrated using the Cu2p3/2 feature at $932.6 \pm 0.1\text{ eV}$ and Au 4f at $83.9 \pm 0.1\text{ eV}$ for known standards. The sample experienced variable degrees of charging. The binding energy scale was referenced using the C1s line at 284.8 eV. The samples were analyzed after a base pressure of 2×10^{-9} mbar was reached within the analysis chamber. Data processing was performed with the XPS peak program. The spectra were decomposed with the least squares fitting routine provided with the software, with a Gauss/Lorentz product function and after subtracting a Shirley background. Atomic ratios were calculated from the peak areas using sensitivity factors provided with the data system and background subtraction. HRTEM was observed with TOPCON 002B (Topcon Co.) at 120 kV. For the observations, the samples were dispersed in ethanol and a small amount of the dispersion solution was dropped on copper grids covered with holy carbon membrane and dried naturally. The thermogravimetric analysis was

performed using a TGA Q500 instrument by TA Instrument, under an inert atmosphere of nitrogen, with a rate of $10^{\circ}\text{C min}^{-1}$, and the weight changes were recorded as a function of temperature. Steady-state absorption spectra in the visible region were measured on a Shimadzu UV 3600 spectrometer. Steady-state fluorescence spectra were measured on a Shimadzu RF-5300PC spectrofluorophotometer. The electrochemical measurements were carried out with an Autolab PGSTAT 30 potentiostat, using a BAS MF-2062, Ag/AgNO₃ reference electrode, an auxiliary electrode consisting of a Pt wire and a Metrohm 6.1247.000 conventional glassy carbon electrode (3 mm o.d.) as a working electrode in *o*-dichlorobenzene/acetonitrile (4:1) containing 0.1 M (n-Bu)₄NPF₆. A 10 mL electrochemical cell from BAS, Model VC-2 was also used. The solution was purged with Argon for at least 15 min before measurements. The scan rates were 100 mV. All of the solutions were purged prior to spectral measurements by using Ar-gas. Experiments were performed at room temperature.

Laser flash photolysis spectroscopy (LFP)

Laser flash photolysis experiments were carried out using the third (355 nm) harmonic of a Q-switched Nd:YAG laser (Spectron Laser Systems, UK; pulse width ca. 9 ns and 35 mJ pulse⁻¹). The signal from the monochromator/photomultiplier detection system was captured by a Tektronix TDS640A digitizer and transferred to a PC that controlled the experiment and provided suitable processing and data storage capabilities.

Femtosecond spectroscopy

The TA spectra were recorded using a typical pump–probe system. The femtosecond pulses were generated with a compact regenerative amplifier that produces pulses centered at 800 nm (~100 fs, 1 mJ/pulse). The output of the laser was splitted into two parts to generate the pump and the probe beams. Thus, tunable femtosecond pump pulses (240- 1600 nm) were obtained by directing the 800 nm light into an optical parametric amplifier. In the present case, the pump

was set at 400 nm and was focused onto a rotating cell containing the solutions under study after passing through a chopper. The white light used as probe was produced after part of the 800 nm light from the amplifier travelled through a computer controlled 8 ns variable optical delay line and impinge on a CaF₂ rotating crystal. This white light is in turn splitted in two identical portions to generate reference and probe beams that then are focused on the rotating cell containing the sample. In turn, the pump and the probe are made to coincide to interrogate the sample. A computer controlled imaging spectrometer is placed after this path to measure the probe and the reference pulses and obtain the transient absorption decays/spectra.

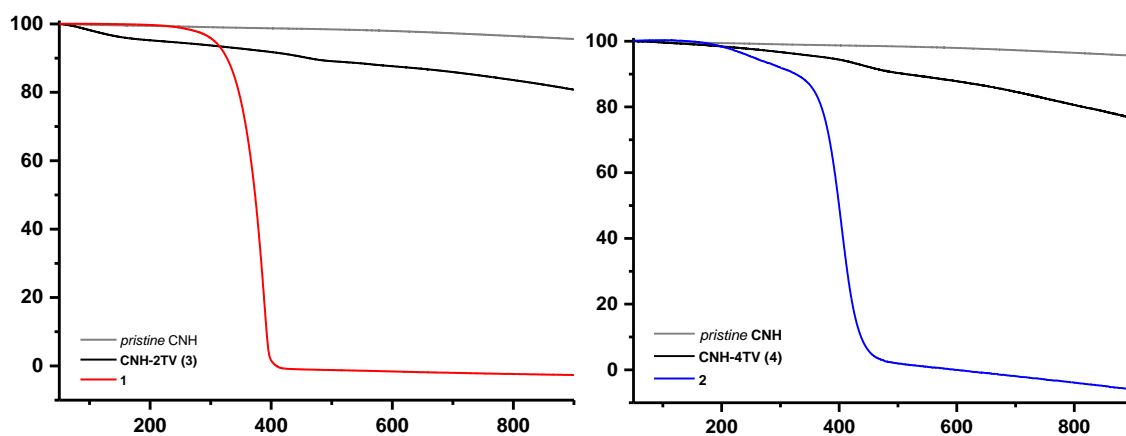


Figure S1. TGA graphs of (left) *pristine* CNH (gray) compared with *functionalized 3* (black) and its precursor oligomer 2TV (**1**) (red) and (right) *pristine* CNH (gray) compared with *functionalized 4* (black) and its precursor oligomer 4TV (**2**) (blue). All thermographs obtained under nitrogen atmosphere.

Table S1. Functionalization data based on TGA and Raman results.

Sample <i>f</i> -CNH	TGA weight loss (%)	Functional group coverage ^a	Raman D/G ratio ^{b, c}
3	10	423	1.71
4	9	876	1.25

^a Number of carbon atoms per functional group ^b Calculated I_D/I_G ratios from Raman spectra. ^c Raman I_D/I_G ratio for *pristine* CNH = 1.06

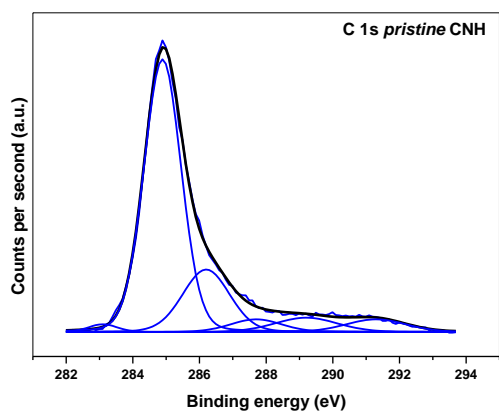


Figure S2. C 1s high-resolution core level spectra of *pristine* CNH.

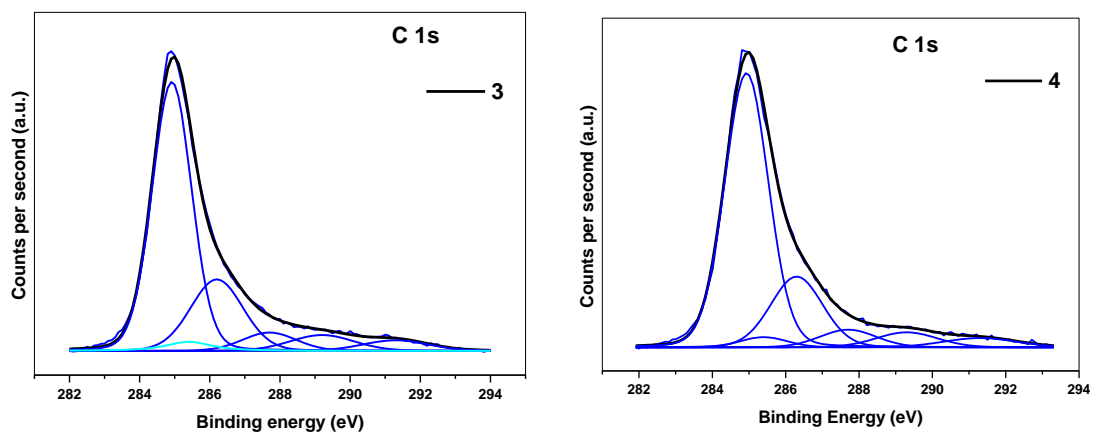


Figure S3. C 1s high-resolution core level spectra of **3** and **4**.

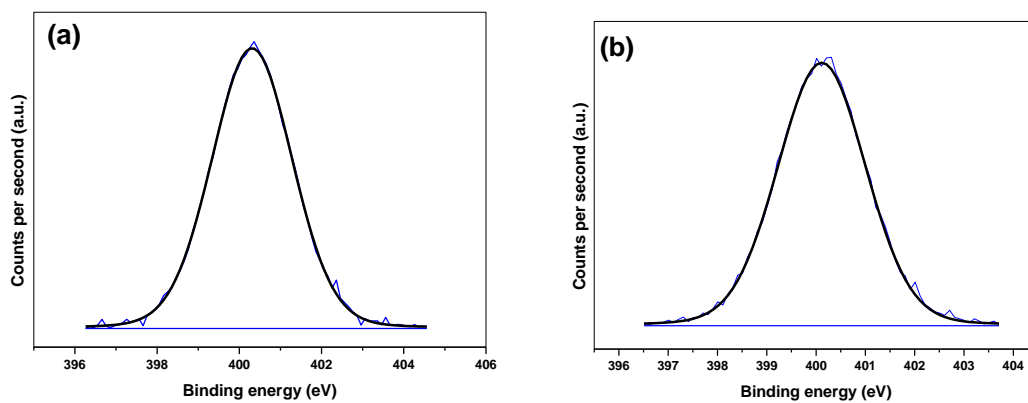


Figure S4. N 1s high-resolution core level spectra of (a) **3** and (b) **4**.

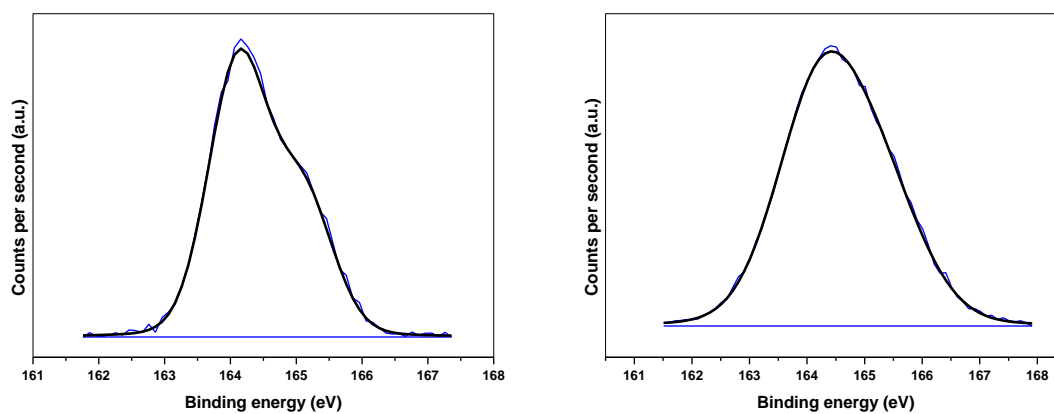
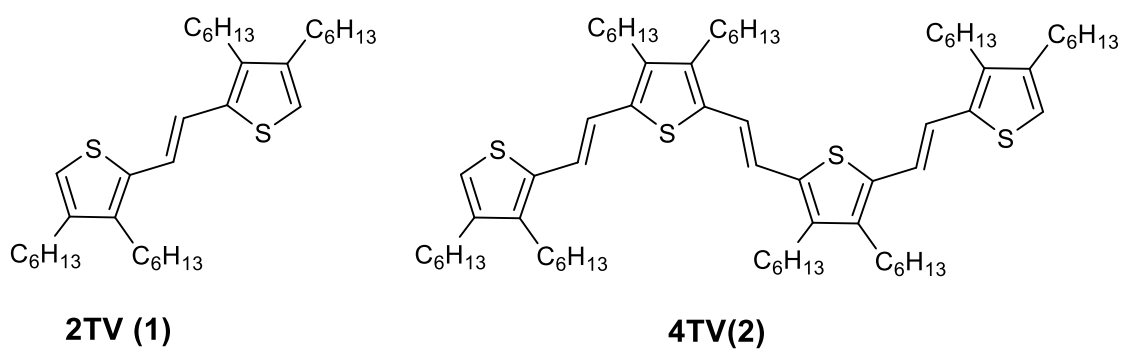


Figure S5. S 2p high-resolution core level spectra of (a) **3** and (b) **4**.

Table S2. Binding energies (eV) of *pristine CNHs* and *functionalized* samples **3** and **4**. In parentheses are peak percentages.

Sample	BE (ev) C 1s (%)							BE (ev) O 1s (%)		BE (ev) N 1s (%)	BE (ev) S 2p (%)
	sp ² C	sp ³ C	C-O	C=O	COO	$\pi-\pi^*$	C-N**	O-C	O=C	N-C	S-C
<i>pristine CNHs</i>	284.8 (68)	-	286.2 (18)	287.7 (4)	289.2 (5)	291.2 (5)	-	533.5 (51)	532.2 (49)	-	-
3	284.8 (58)	285.4 (3)	286.2 (22)	287.7 (6)	289.2 (7)	291.3 (4)	286.2	533.4 (50)	532.0 (50)	400.3	164.1
4	284.8 (64)	285.4 (3)	286.3 (20)	287.7 (5)	289.3 (5)	291.3 (3)	286.3	534.0 (43)	532.6 (57)	400.2	164.2

* C 1s satellite line ** this signal overlaps with that of C-O species.



Scheme S1. Structures of oligothiénylenevinylenes 2TV (**1**) and 4TV (**2**)

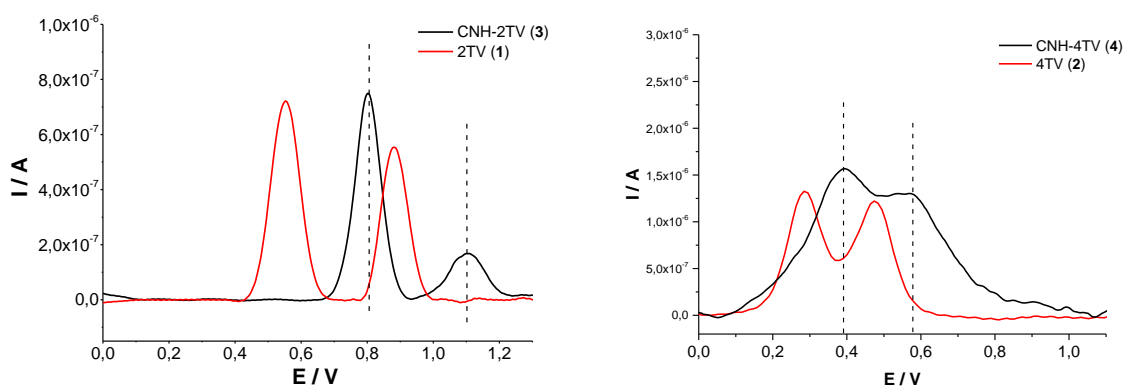


Figure S6. Square wave voltammetry (oxidation run) of the final hybrids **3** and **4** compared to that of control *n*TV **1** and **2**, respectively.

Table S3: Oxidation potentials (OSWV) of oligothiolenylenevinylenes 2TV (**1**) and 4TV (**2**) and *functionalized* CNH **3** and **4** measured at room temperature in *o*-dichlorobenzene (ODCB)/acetonitrile (4:1)^a versus Fc/Fc⁺ (V)

Sample	E ¹ _{ox} (V)	E ² _{ox} (V)
2TV (1)	+0.44	+0.77
4TV (2)	+0.16	+0.35
3	+0.69	+1.01
4	+0.28	+0.45

^a Experimental conditions: V vs Ag/AgNO₃; GCE as working electrode; 0.1 M TBAPF₆; scan rate: 100 mV/s.

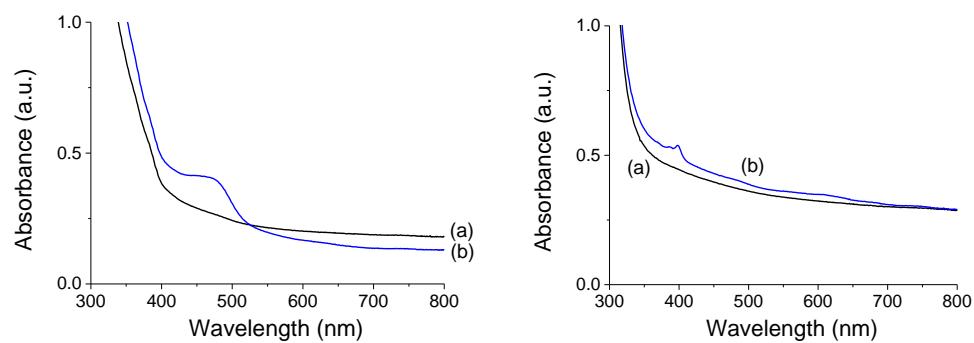


Figure S7. Absorption spectrums of an Ar-purged DMF solution of compound **1** (2TV) containing 50 μ L of a DMF solution of CNH (0.2 mg/mL) (left) and nanohybrid **3** (right) containing both also 100 μ L of MeOH as an electron donor and 50 μ L of a DMF solution of $MVCl_2$ (0.01 M) before (a) and after 355 nm laser excitation (b).

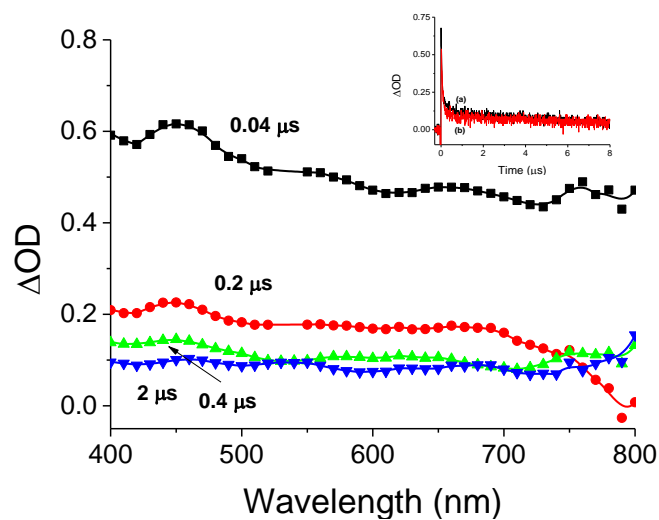


Figure S8. Transient spectra recorded from 40 ns to 2 μ s after 532 nm laser excitation of an Ar-purged DMF solution of nano-hybrid **4**. The temporal profiles of the transient signal monitored at 420 (a) and 550 nm (b) of Ar-purged solutions of **2** (4TV) (inset).

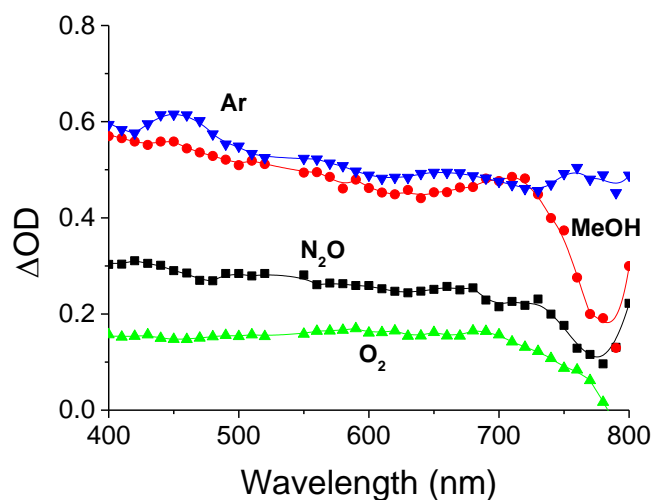


Figure S9. Comparative transient spectra recorded at 40 ns after 532 nm laser excitation of a DMF solution of nano-hybrid **4** after purging with Ar, O₂, N₂O and addition of 100 μ L of MeOH.

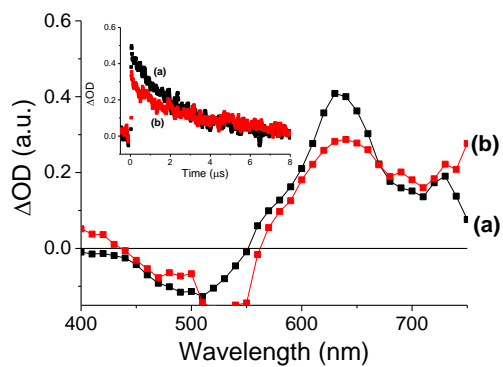


Figure S10. Transient spectra recorded 0.45 μs after 532 nm laser excitation of an Ar-purged DMF solution of 4.5×10^{-5} M of **2** (4TV) before (a) and after (b) the addition of 50 μL of a DMF solution of CNH (0.2 mg/mL). The inset shows the comparative signal decay monitored at 640 nm before (a) and after (b) addition of the CNH solution.